33RD INTERNATIONAL COSMIC RAY CONFERENCE, RIO DE JANEIRO 2013
THE ASTROPARTICLE PHYSICS CONFERENCE

ICRC 2013

GRAINE project : The first demonstration of emulsion gamma-ray telescope in 2011 balloon experiment

SATORU TAKAHASHI[1] FOR GRAINE COLLABORATION: SHIGEKI AOKI[1], KANAME HAMADA[2], TOSHIO HARA[1], KATSUMI ISHIGURO[3], ATSUSHI IYONO[4], KEIKI KAMADA[1], HIROAKI KAWAHARA[3], NOBUKO KITAGAWA[3], KOICHI KODAMA[5], RYOUSUKE KOMATANI[3], MASAHIRO KOMATSU[3], MOTOAKI MIYANISHI[3], FUKASHI MIZUTANI[1], SAKI MIZUTANI[1], KUNIHIRO MORISHIMA[3], NAOTAKA NAGANAWA[3], TATSUHIRO NAKA[3], RYO NAKAGAWA[1], YUJI NAKATSUKA[3], MITSUHIRO NAKAMURA[3], TOSHIYUKI NAKANO[3], KIMIO NIWA[3], KEITA OZAKI[1], HIROKI ROKUJO[3], TAKASHI SAKO[3], YOSHITAKA SAITO[2], OSAMU SATO[3], YOSHIHIRO SATO[6], ATSUMU SUZUKI[1], KAZUYA SUZUKI[3], SATORU TAKAHASHI[1], KEISUKE TAMURA[2], IKUO TEZUKA[6], JUNYA YOSHIDA[3] AND TETSUYA YOSHIDA[2]

[1]*Kobe University,* [2]*ISAS/JAXA,* [3]*Nagoya University,* [4]*Okayama University of science,* [5]*Aichi University of education,* [6]*Utsunomiya University*

satoru@radix.h.kobe-u.ac.jp

Abstract: We are furthering our GRAINE project. This balloon experiment was performed using a telescope with a 12.5cm×10cm aperture area and a 4.3hour (1.6hours@35km) flight duration in 2011. Working tests of each element and connection tests between elements were performed. Atmospheric gamma-ray flux was measured. The first demonstration of an emulsion gamma-ray telescope was described using flight data in our 2011 balloon experiment.

Keywords: cosmic-ray, gamma-ray, telescope, nuclear emulsion

1 Introduction

We are furthering the project of 10MeV-100GeV cosmic gamma-ray observation, with precise (0.08deg@1-2GeV) and polarization sensitive large aperture area ($\sim$10m^2) emulsion telescope by repeating long duration balloon flights [1]. We call this project GRAINE (Gamma-Ray Astro-Imager with Nuclear Emulsion). For the first step, a balloon experiment was performed using a telescope with 125cm^2 aperture area and 4.3hour (1.6hours@35km) flight duration for working tests of each element, connection tests between elements and measurement of atmospheric gamma-rays. As the next step, a balloon experiment is planned with 2500cm^2 aperture area and 1day flight duration for overall test by detecting known bright gamma-ray source and the observation with the highest imaging resolution. As a future step, scaling up aperture area and flight duration, full-scale observations are planned.

In this paper, the first demonstration of an emulsion gamma-ray telescope is described using flight data in our 2011 balloon experiment.

2 Balloon experiment in 2011

The balloon experiment was done at Taiki Aerospace Research Field (TARF) [2] in Hokkaido, Japan on 8th June 2011. Emulsion chamber, star camera, thermo meters, pressure meter, GPSs and battery were mounted on the gondola. The balloon was launched at 5:04 Japan Standard Time. Level flight at 34.7km altitude and 6.5hPa residual atmospheric pressure (6.6g/cm^2 atmospheric depth) was initiated at 7:14. System shutdown was 8:40. The gondola was cut off at 8:50. The gondola splashed down on the sea at 9:24. The gondola was recovered successfully at 9:43. Total flight duration was 4.3 hours. Of the 4.3 hours, 1.6 hours was of level flight at 34.7km altitude.

3 Emulsion chamber

Fig.1 shows the structure of the emulsion chamber. An emulsion chamber with 12.5cm×10cm aperture area consisting of a converter, timestamper and calorimeter. Emulsion films were held with adhesive tape and mechanical support. Converter consisted of a stack of 98 OPERA films (293μm thick) [3], 4 high sensitivity emulsion gel films (170μm thick) [4] and 91 copper foils (50 μm thick). Total thickness of converter was 35.0mm. Total radiation length was 0.54 radiation lengths (Xo) corresponding to 0.34 conversion efficiency. Timestamper consisted of multi-stage shifter co-developed with Mitaka Kohki Co., Ltd. based on our invention and its demonstration [5]. The 3rd film on the 3rd stage of the multi-stage shifter was a high sensitivity emulsion gel film. More details and a demonstration using flight data is described in [6]. Calorimeter consisted of a stack of 32 OPERA films, 10 lead plates (0.5mm thickness) and 17 lead plates (1.0mm thickness). Total thickness and radiation lengths was 31.9mm and 4.0Xo, respectively.

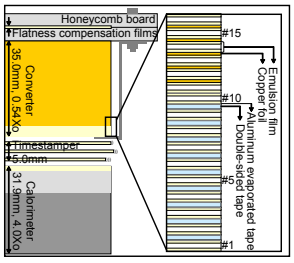

Fig. 1: The structure of emulsion chamber is shown (side view). Emulsion chamber consists of converter, timestamper and calorimeter. Converter films were numbered from bottom to top.

4 Converter

4.1 Readout and reconstruction of emulsion tracks

Emulsion tracks were read out by automatic emulsion scanning system SUTS [7]. Scanning area was varied to find optimum condition. Finally, scanning area was set with 0.0mm, 0.5mm, 1.0mm and 1.5mm inside from each edge of the film. Angle acceptance for track recognition was set with $|\tan\theta_{proj}| < 1.0$ where θ_{proj} is projection angle for normal vector at the emulsion film surface. The number of readout tracks per emulsion layer is $\sim 10^9$ tracks. Out of these tracks, $10^2 - 10^3$ beginning tracks of electron pairs were expected.

Readout tracks were reconstructed. Fig.2 shows the number of tracks from film#1 to #16 for each step. Readout tracks were clustered for each scanned layer. Clustered tracks were connected between both sides of the base in a film (base track). Base tracks were connected between films. Connection allowance between films was set with angle dependence. With this allowance, tracks with $|\tan\theta_{proj}| <$ 1.0 were connected. Connection allowance was also set considering multiple coulomb scattering for low momentum tracks. With this allowance, tracks down to 25MeV/c were connected. To get around the track inefficiency in a film, track connections between films were performed every 2 films in maximum. Tracks connected between films were folded in, all connected films. From film#1 to #16, 8.7×10^7 tracks were folded in. More details of track reconstruction are described in [8][9].

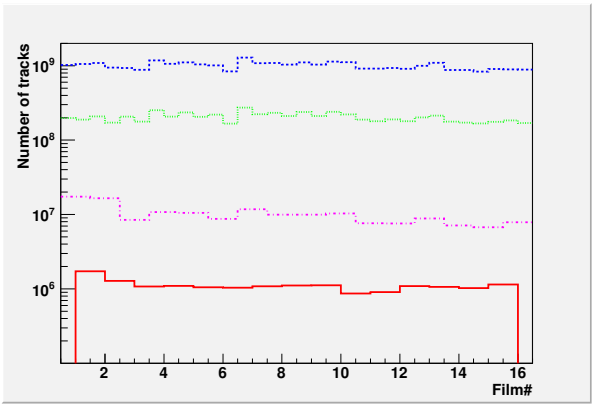

Fig. 2: The number of tracks from film#1 to #16 for each step is shown. Dashed line shows the number of readout tracks. Dotted line shows the number of clustered tracks. Dot-dashed line shows the number of connected tracks between both sides of the base in a film. Solid line shows the number of connected tracks between adjacent film.

The accuracy of track connection between films was evaluated. Fig.3 (top) shows the distributions of position difference and angle difference in a projection. Gaussian fitted σs were obtained as 0.75μm and 4.2mrad at $\tan\theta$ <0.1 where θ is incident angle. Fine accuracy was obtained for the whole area of an emulsion film. Fig.3 (bottom) shows the distributions of obtained σs for connected films. Fine accuracy was obtained for all connected films.

The track detection efficiency in an emulsion film was evaluated. Fig.4 (top-left) shows the position distribution of the efficiency in a film. Uniform efficiency was obtained

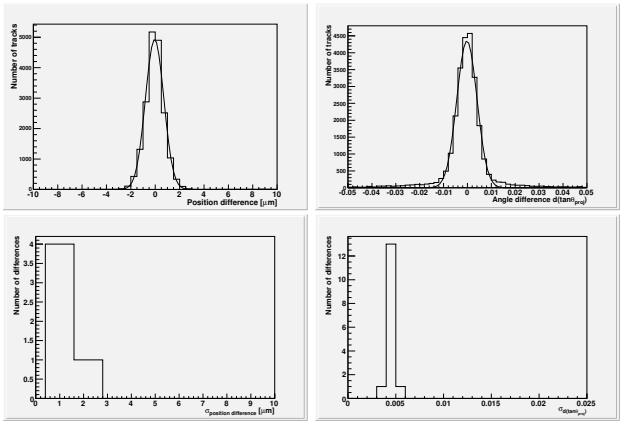

Fig. 3: The distributions of position difference (top-left) and angle difference (top-right) in a projection with gaussian fitted curve. (film"#12 – #13", $\tan\theta$<0.1) The distributions of position difference σs (bottom-left) and angle difference σs (bottom-right) for connected films (film"#1 – #2" to "#15 – #16", $\tan\theta$<0.1).

over the whole area of the film. Fig.4 (top-right) shows the distribution of the efficiency for all connected films. Uniform efficiency was obtained for all connected films. Fig.4 (bottom) shows the efficiency as a function of incident angle. The efficiency obtained was 78% at $\tan\theta$<0.1 and 64% at 1.0<$\tan\theta$<1.1. By setting the allowance dependent on the incident angle in base track reconstruction, track efficiency of 95% at 1.0<$\tan\theta$<1.1 was achieved. By using the high sensitivity emulsion gel film as the 3rd film on the 3rd stage of the multi-stage shifter, higher efficiency and higher uniformity for each incident angle was achieved.

4.2 The detection of gamma-ray events

From 8.7×10^7 reconstructed tracks, gamma-ray events were systematically searched for using criteria of electron pair topology. Out of the reconstructed tracks, 2.3×10^5 tracks were selected as the downward starting tracks from film#7. Out of these tracks, 1.1×10^3 events were selected as events having a partner track which was downward starting from film#7 or below, within 75μm and 75mrad at the start of the track segment. Out of these events, 153 events were selected as gamma-ray events by checking the event display. Fig.5 shows one of the detected gamma-ray events. The detection of clear gamma-ray events was achieved.

The detection efficiency of gamma-ray events was evaluated using Monte Carlo simulation. Fig.6 shows the detection efficiency as a function of gamma-ray energy for each criteria. The solid line shows the detection efficiency found in this analysis. The dashed line shows the detection efficiency of additional searchings for events with larger openning angles. The dotted line shows the detection efficiency using emulsion films with higher track detection efficiency, like the high sensitivity emulsion gel films installed in a part of the chamber in this flights. By using high performance emulsion films, the detection efficiencies can be achieved up to 70% at 100MeV and up to 90% at 200MeV in subsequent flight.

The reliability of detected gamma-ray events was evaluated combined with timestamper. Gamma-ray events were detected with a reliability of 97%.

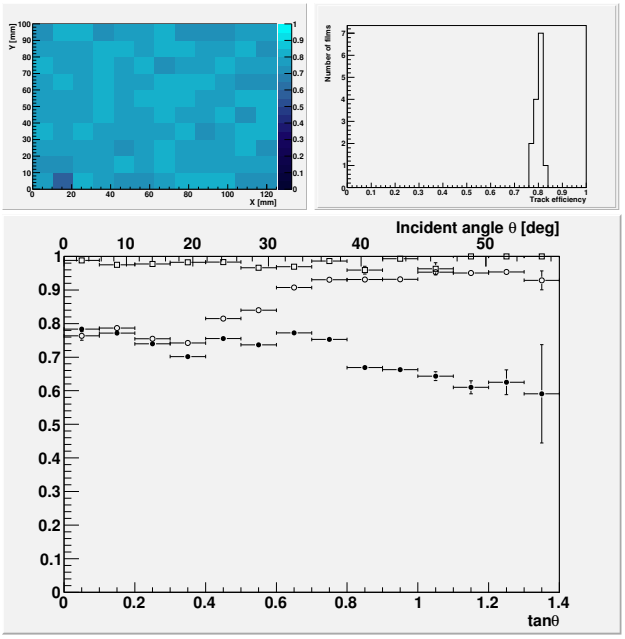

Fig. 4: (left) The position distribution of the track detection efficiency in an emulsion film (film#5, $\tan\theta<0.1$). (right) The distribution of the track detection efficiency for whole connected films (film#2 to #15, $\tan\theta<0.1$). (bottom) The track detection efficiency as a function of incident angle. Filled circles shows the efficiency (film#5). Open circles shows the efficiency which has the allowance with incident angle dependence in base track reconstruction (film#5). Open boxes shows the efficiency of high sensitivity emulsion gel film (3rd film on 3rd stage of multi-stage shifter, 5mm×5mm).

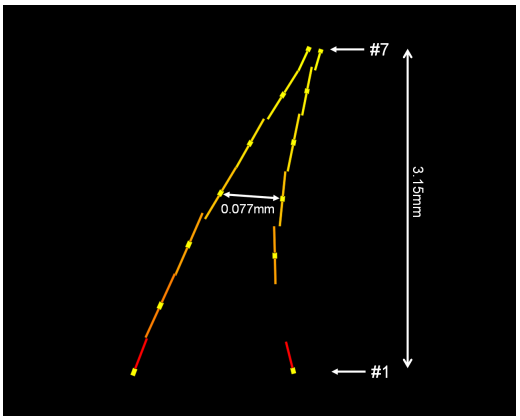

Fig. 5: The one of gamma-ray events detected and reconstructed energy. Incident angle of the event is 9.75deg. A left side track was measured as 60^{+20}_{-12}MeV/c corresponding to 25% relative error for inverse momentum. A right side track was also measured as 32^{+9}_{-6}MeV/c corresponding to 22% relative error for inverse momentum. From the momenta, the gamma-ray energy was reconstructed as 92^{+22}_{-13}MeV corresponding to 24% relative error to plus side and 14% relative error to minus side.

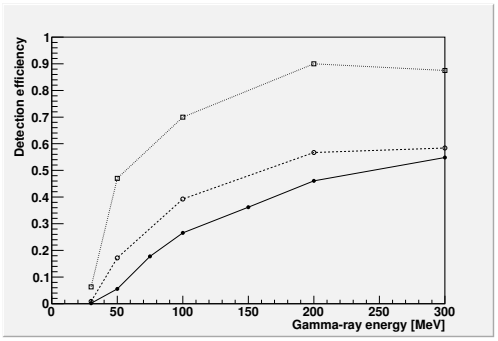

Fig. 6: The detection efficiency of gamma-ray events (normal incidence, 7 films used) is shown as a function of gamma-ray energy for each criteria. The solid line shows the detection efficiency in this analysis. The dashed line shows the detection efficiency in additional searching for events with larger openning angle. The dotted line shows the detection efficiency in using the emulsion films with higher track detection efficiency (100%) like high sensitivity emulsion gel films installed in a part of the chamber in this flight.

Systematic energy reconstrunction was tried for the detected gamma-ray events. By measuring the momenta of an electron pair with multiple coulomb scattering, the gamma-ray energy can be reconstructed. Fig.5 shows the one of gamma-ray events reconstructed energy. In this analysis, for 306 tracks of 153 events, systematic momentum measurement and gamma-ray energy reconstruction were tried. Out of 153 events, 112 events corresponding to 73% were reconstructed the gamma-ray energy. The others 41 events corresponding to 27% were set the lower limit of the gamma-ray energy. By using the calorimeter located at the bottom part, measurement accuracy can be improved and events with a lower limit can be recovered. In this analysis, the detection of gamma-ray events was performed down to around 50MeV region.

4.3 The derivation of atomospheric gamma-ray flux

Atmospheric gamma-ray flux was derived. Fig.7 shows derived integral flux at 6.6g/cm^2 atmospheric depth compared with previous measurement [10]. Derived gamma-ray flux was consistent with previous measurement.

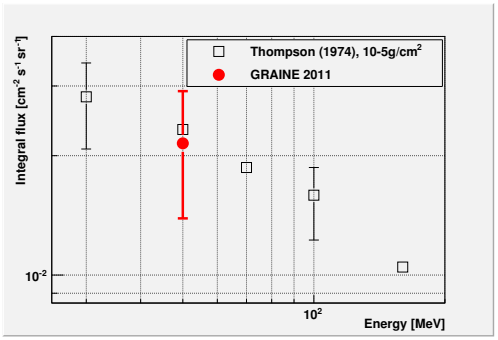

Fig. 7: Derived atmospheric gamma-ray flux (filled circle) and previous measurement (open box) are shown.

5 Timestamper

Multi-stage shifter as timestamper well worked during balloon flight and timestamped to emulsion tracks with 0.1s accuracy[6]. By requiring tracks within $\pm$0.5s time window for gamma-ray event timestamp with timestamper and by requiring convergent tracks with converter, hadron interaction events with gamma-ray events were detected. Then gamma-rays produced in converter were distinguished. Fig.8 shows the one of detected hadron interaction events with gamma-ray events. The detection of hadron interaction events with gamma-ray events can not only suppressed background, but also can be used as calibration source (pointing accuracy, energy, polarization and detection efficiency). Space angle difference between the line of primary vertex to conversion point and the gamma-ray direction reconstructed from electron pair was obtained as 0.65deg (0.0114rad) for 45^{+33}_{-10}MeV gamma-ray energy and for 46.61deg incident angle. Reasonable value was obtained and the evaluation procedure of pointing accuracy was established for each energy and each incident angle with a flight data.

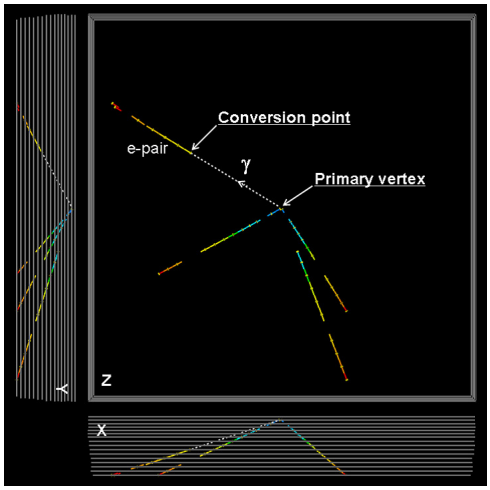

Fig. 8: The one of detected hadron interaction events with gamma-ray events is shown with 1.2cm$\times$1.2cm$\times$16films converter region. The gamma-ray event timestamp is 7:18:34.5 (local time). Primary vertex and conversion point were confirmed by eye check with a microscope.

6 Attitude monitor

Star camera as attitude monitor worked at 34.7km level flight in daytime. Attitude monitoring was performed with enough accuracy. Then attitude determination combined with timestamper was achieved with enough accuracy ($<$0.02deg) [11]. Detected gamma-ray events at converter were timestamped at timestamper. By combining attitude monitor information, gamma-ray direction was determined on celestial coordinates. Fig.9 shows the first light event. The procedure of gamma-ray pointing on celestial coordinates was established and the first light was performed as GRAINE project.

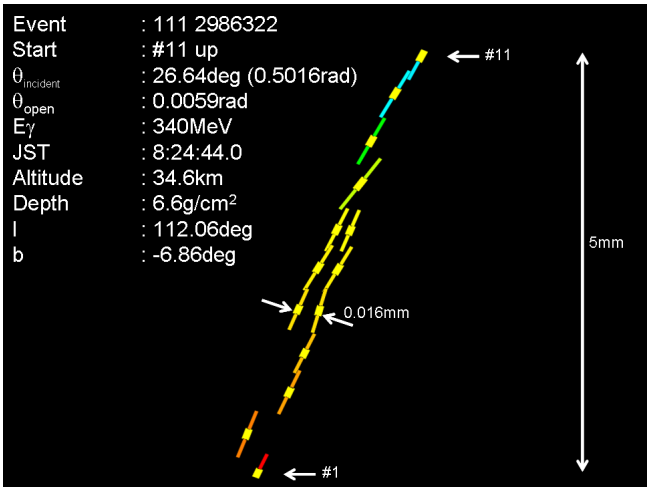

Fig. 9: The first light event is shown. "l" and "b" are galactic longitude and galactic latitude determined by gamma-ray pointing procedure.

7 Summary

We are promoting GRAINE project. The balloon experiment was performed with 12.5cm$\times$10cm aperture area and 4.6hours flight duration in 2011. Each element and connection between elements were demonstrated with the flight data. Atmospheric gamma-ray flux was measured. Next balloon experiment is planned on JAXA international scientific ballooning at Alice Springs, Australia in 2014. With 2500cm^2 aperture area and 24hours flight duration, overall test will be done by detecting known bright gamma-ray source. Then the observation will be performed with highest imaging resolution around 100MeV region.

Acknowledgment: This work was supported by JSPS KAKENHI Grant Number 20244031 and Grant-in-Aid for JSPS Fellows. This manuscript was corrected by D.Moore on KALCS program.

References

[1] S. Aoki et al., arXiv:1202.2529; S. Aoki et al., Proc. of 29th International Symposium on Space Technology and Science, Nagoya (2013); S. Takahashi et al., Proc. of 33rd International Cosmic Ray Conference, Rio De Janeiro (2013).
[2] H. Fuke et al., Advances in Space Research 45 (2010) 490-497.
[3] T. Nakamura et al. Nucl. Instr. and Meth. A 556 (2006) 80.
[4] N. Naganawa and K. Kuwabara, Abstracts for SPIJ's Annual Conference in 2013, Chiba (in Japanese).
[5] S. Takahashi, et al., Nucl. Instr. and Meth. A 620 (2010) 192.
[6] H. Rokujo et al., Nucl. Instr. and Meth. A 701 (2013) 127.
[7] K. Morishima and T.Nakano, JINST 5 P04011 (2010).
[8] N. Nonaka, Ph.D. Thesis, Nagoya University, Japan, 2002 (in Japanese); K. Kodama, et al. Nucl. Instr. and Meth. A 493 (2002) 45
[9] K. Hamada et al., JINST 7 P07001 (2012).
[10] D. J. Thompson, J. Geophys. Res. 79, 1309 (1974).
[11] K. Ozaki et al., Proc. of Balloon Symposium, ISAS/JAXA (2007) isas12-sbs-022 (in Japanese).